

# Theoretical Aspects of Gamma-Ray Bursts

Andrei M. BELOBORODOV

*Physics Department, Columbia University, 538 W. 120th Street, New York, 10027,  
USA*

(Received )

Cosmological GRBs are discussed with an emphasis on their plausible connection with black holes. GRBs can be triggered by collapse of stellar-mass objects that leads to formation of a black hole and a transient debris disk with a huge accretion rate. The disk is believed to produce a relativistic jet (“fireball”) that expands and emits to infinity the observed burst of gamma-rays. This accretion-jet picture is similar to quasars and X-ray binaries, however, there are important differences: the physical conditions and the cooling mechanism in the disk are very different. The observed radiation is emitted when the expanding fireball becomes transparent, at distances much larger than the Schwarzschild radius. The burst is then observed as a powerful relativistic explosion and the transient accretion disk in its center serves as a brief source of energy that drives the explosion. The explosion picture depends on the fireball nuclear composition which is shaped close to the black hole. A large amount of free neutrons survive till the emission phase and link the physics of the central engine to observed radiation.

## §1. GRB Explosions and Black Holes

Gamma-ray bursts (GRBs) occur every day in the sky and last typically seconds or minutes. The energy spectrum of the burst peaks at 0.1-1 MeV, and the truly unique feature of this phenomenon is its huge luminosity: the energy comparable to (or even exceeding) a supernova is emitted in just seconds. By contrast, a normal supernova light peaks on a week timescale: the exploding star has to expand enough to become transparent, so that its thermal energy can be radiated away, and this takes  $\sim 10^6$  s. The short duration of GRBs implies that the mass of the emitting material  $M$  is much smaller than a stellar mass.

Moreover,  $Mc^2$  is far below the burst energy  $E$ , so we deal with a *relativistic* explosion: the emitting plasma should develop a Lorentz factor  $\Gamma \sim E/Mc^2 \gg 1$ . Detailed calculations show that the GRB durations can be reconciled with their energies if  $\Gamma > 100$ .<sup>1)</sup> For such a high  $\Gamma$  the observed duration  $t_{\text{obs}}$  is strongly reduced by the Doppler effect compared to the emission in the local frame:  $t_{\text{obs}} = (1 - v/c)t_{\text{em}} \approx (t_{\text{em}}/2\Gamma^2)$ .

The burst takes place in an ambient medium, and hence the relativistic ejecta must decelerate as they sweep up enough ambient material. The energy dissipated in this deceleration gives rise to the observed afterglow emission. As  $\Gamma$  decreases with increasing radius  $R$  the afterglow radiation is emitted on longer timescales  $t_{\text{obs}} \sim (R/c\Gamma^2)$  and in softer bands.

Thus, a phenomenological picture of the GRB emerged: a highly relativistic ejecta (fireball) emits the prompt  $\gamma$ -ray emission of short duration, which is followed by the afterglow from the deceleration stage. The main emission mechanism is syn-

chrotron which requires the presence of magnetic fields and nonthermal electrons in the explosion. This aspect of GRB theory is poorly understood; it involves complicated plasma physics and contains a number of unknown parameters. Therefore, the derivation of the explosion parameters from the data is ambiguous and the nature of the circumburst medium (interstellar medium? progenitor wind?) is still disputed. It is also unclear whether the ejecta are dominated by baryons (flux of kinetic energy) or magnetic field (Poynting flux).

There is a growing observational evidence that GRBs are produced by massive-star progenitors, most likely of Wolf-Rayet type. In some cases, a supernova component has been detected in the afterglow, with the most impressive case of GRB 030329.<sup>3)</sup> The suspected supernovae are of type Ic, which are also associated with black hole formation.

Observational constraints on the trigger mechanism are inferred from the temporal variability and the energy budget of GRBs. The prompt  $\gamma$ -radiation is strongly variable on timescales  $\delta t$  ranging from milliseconds to the overall duration of the burst. In other words, the emitted radiation front is spatially inhomogeneous on scales  $10^7 \lesssim c\delta t \lesssim 10^{11}$  cm. If the front was emitted by the ejecta, they should have a radial structure on scales  $10^7 \lesssim \delta R \lesssim 10^{11}$  cm. The high- $\Gamma$  outflow is causally disconnected on scales  $\delta R > R/\Gamma^2 = 10^7 R_{12}(\Gamma/300)^{-2}$  cm, so it was likely created inhomogeneous: the central engine was unsteady on timescales as short as milliseconds. This indicates that the size of the central engine does not exceed  $10^7$  cm. Known objects of this size, which are capable to release energies above  $10^{51}$  erg, are black holes or neutron stars.

Most of the proposed scenarios are based on the gravitational source of energy.<sup>2)</sup> It can be a neutron-star merger, a collapse of a rotating massive star (“collapsar”), or a delayed collapse of a spinning neutron star (“supranova”), all of which lead to the formation of a black hole and an accretion disk of debris. GRBs can also be produced by just born neutron stars, however, we shall focus here on the accretion scenario as it is directly related to the subject of this meeting: black holes.

A relativistic explosion will be produced if the accretion disk creates a relativistic jet. This seems likely to happen given that jets are observed in other black-hole objects — X-ray binaries and quasars. The jet can be fed by the Blandford-Znajek process that extracts the spin energy of the black hole. It can also be a MHD outflow from the disk.<sup>4),5)</sup> The precise mechanism still remains to be established, and this is especially difficult in the context of GRBs where the central engine is hidden from direct observation by its optically thick ejecta.

A different aspect of GRBs, which is easier to understand, is the nuclear history of the burst. It turns out to play important role in the overall picture of the explosion: the GRB resembles a huge neutron bomb. Below we discuss the physical conditions in GRB accretion disks, then address the nuclear aspect of this phenomenon and its connection with the mechanism of observed emission.

## §2. Hyper-Accretion

A disk with accretion rate  $\dot{M}$  can power a relativistic outflow (fireball) with luminosity

$$L = \epsilon_f \dot{M} c^2 \approx 10^{51} \left( \frac{\epsilon_f}{0.01} \right) \left( \frac{\dot{M}}{10^{32} \text{g/s}} \right) \text{ erg s}^{-1}, \quad (2.1)$$

where  $\epsilon_f$  is the efficiency of  $\dot{M}c^2$  conversion into a fireball. This picture is similar to accreting black holes in X-ray binaries, and the standard theory of disk accretion applies.<sup>6)-9)</sup> However,  $\dot{M}$  is some 15 orders of magnitude higher, which leads to important differences:

1. The disk, its corona, and the jet are in perfect blackbody state because of their high densities and temperatures. The rates of photon emission and absorption are huge, the radiation maintains detailed equilibrium and has a Planckian spectrum everywhere near the black hole. Given the liberated power  $L \sim 10^{52} - 10^{54} \text{ erg s}^{-1}$  and the size of the engine  $\sim 10^6 - 10^7 \text{ cm}$ , one finds the blackbody temperature,

$$kT \sim 1 - 10 \text{ MeV}. \quad (2.2)$$

2. At such temperatures, an equilibrium population of  $e^\pm$  pairs must be present. The rates of pair annihilation and creation by photon-photon interactions are huge, and the  $e^\pm$  maintain a perfect Fermi-Dirac distribution with the occupation number

$$f_\pm(E) = \frac{1}{\exp[(E \pm \mu)/kT] + 1}, \quad (2.3)$$

where  $\mu \equiv \mu_- = -\mu_+$  is the electron chemical potential (thermodynamic equilibrium of  $e^\pm$  with radiation implies  $\mu_+ + \mu_- = 0$ .)

3. The disk density  $\rho \gtrsim 10^{10} \text{ g cm}^{-3}$  is some 15 orders of magnitude higher than in X-ray binaries. Matter with such densities has the Fermi energy level

$$E_F = 3m_e c^2 \left( \lambda^3 Y_e \frac{\rho}{m_p} \right)^{1/3} \sim 10 \text{ MeV}, \quad (2.4)$$

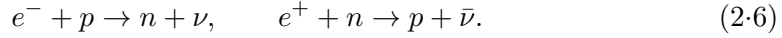
where  $Y_e = n_p/(n_n + n_p)$  and the charged fraction of baryons and  $\lambda = \hbar/m_e c$ .  $E_F$  is comparable to the mean thermal energy of the electrons  $3kT$  and hence the GRB disks are mildly degenerate. The chemical potential is then given by

$$\frac{\mu}{3kT} = \left( \frac{E_F}{3kT} \right)^3, \quad \mu \lesssim 3kT. \quad (2.5)$$

Even mild degeneracy suppresses significantly the positron density,  $f_+/f_- < 1$  (eq. 2.3), because the levels of typical thermal energies  $\sim 3kT$  are significantly occupied by the ambient  $e^-$ , and the creation of new pairs is limited to the free levels. So, the positron density in the disk is modest despite its high temperature.

4. Both  $3kT$  and  $\mu$  exceed the difference between the neutron and proton rest-masses,  $m_n c^2 - m_p c^2 = 1.3 \text{ MeV}$ . Therefore the electrons are energetic enough for the

neutronization reaction — the  $e^-$  capture onto protons.  $e^+$  capture onto neutrons also takes place,



These reactions rapidly convert protons into neutrons and neutrons back into protons, and establish an equilibrium  $Y_e = n_p/(n_n + n_p)$ . Since the positron density is suppressed by degeneracy, the reaction  $e^- + p \rightarrow n + \nu$  is preferential and the equilibrium is shifted to a higher neutron density ( $Y_e < 0.5$ ). Precisely the same mechanism drives neutronization in the core of a supernova collapse, leading to formation of neutron stars.

5. The material around the black hole has a huge optical depth for photons, and radiation diffusion is completely negligible on the accretion timescale. The only cooling mechanism of the disk is neutrino emission. Reactions (2.6) are the main channels of neutrino emission (although there are also other channels, e.g.  $e^+ + e^- \rightarrow \nu + \bar{\nu}$ ). Thus, the  $e^\pm$  capture reactions regulate both the temperature and the nuclear composition of the accretion disk.

An upper bound on the disk temperature is derived from assumption that the disk does not lose the dissipated energy and instead traps it and advects. The advective flow at a radius  $r$  has energy density<sup>9)</sup>  $w \approx (3/8)(r_g/r)\rho c^2$ , where  $r_g = 2GM/c^2$  is the Schwarzschild radius of the black hole. The energy density in such an advective hot flow is dominated by radiation and weakly degenerate  $e^\pm$ , so that

$$\frac{11}{4}aT_{\max}^4 \approx \frac{3r_g}{8r}\rho c^2, \quad (2.7)$$

where 11/4 accounts for the contribution of relativistic weakly degenerate  $e^\pm$ . Neutrinos make a noticeable contribution to the energy density if they are thermalized (self-absorbed), and then  $T_{\max}$  will be slightly lower. Equation (2.7) yields

$$kT_{\max} \approx 13 \left( \frac{\rho}{10^{11} \text{g cm}^{-3}} \right)^{1/4} \left( \frac{r}{3r_g} \right)^{-1/4} \text{ MeV}. \quad (2.8)$$

The actual disk temperature  $T$  can be lower because of the neutrino cooling, whose efficiency depends on  $\dot{M}$ .

One can show that the rates of reactions (2.6) are sufficiently high to establish an equilibrium  $Y_e$ , i.e. the GRB accretion disks reach  $\beta$ -equilibrium. This is easy to see for disks cooled efficiently by neutrino losses. Indeed, the mean energy of emitted neutrinos,  $E_\nu \lesssim 30$  MeV, is below the liberated accretion energy per nucleon,  $\sim 100 - 300$  MeV, so the efficient cooling implies that more than one neutrino per nucleon is produced, and hence the equilibrium  $Y_e$  is achieved.

In the opposite, advective, regime with  $T \approx T_{\max}$  the disk is weakly degenerate, and the rates of  $e^\pm$  capture in the zero order in  $\mu/kT$  are

$$\dot{n}_{e-p} \approx 1.5 \times 10^{-2} n_p \theta^5, \quad \dot{n}_{e+n} \approx 1.5 \times 10^{-2} n_n \theta^5, \quad (2.9)$$

where  $\theta = kT/m_e c^2$ . The neutronization timescale is  $t_n = n_p/\dot{n}_{e-p} \approx 70\theta^{-5}$  s should

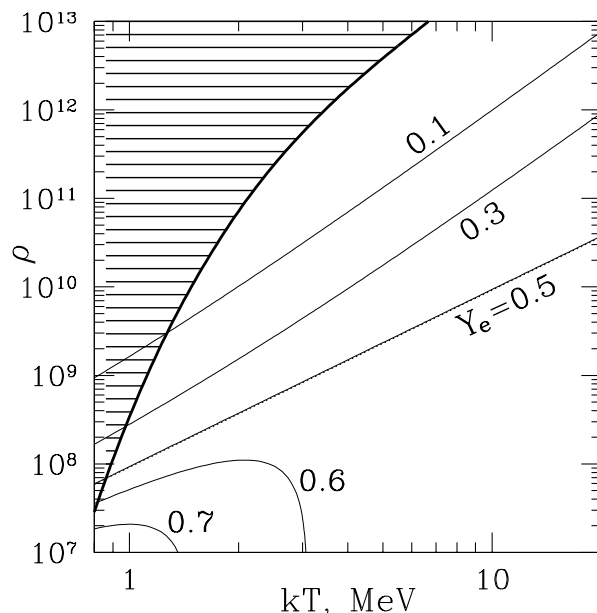


Fig. 1. Contours of equilibrium  $Y_e = n_p/(n_n + n_p)$  on the  $T$ - $\rho$  plane for  $\nu$ -transparent matter.<sup>9)</sup> Composite nuclei dominate in the shaded region.

be compared with the accretion timescale<sup>9)</sup>  $t_a$ ,

$$\frac{t_n}{t_a} \approx 2 \times 10^{-2} \left( \frac{r}{3r_g} \right)^{13/8} \left( \frac{\alpha}{0.1} \right)^{9/4} \left( \frac{M}{M_\odot} \right)^{3/2} \left( \frac{\dot{M}}{10^{32}} \right)^{-5/4}. \quad (2.10)$$

Disks with

$$\dot{M} > \dot{M}_{\text{eq}} \approx 10^{31} \left( \frac{r}{3r_g} \right)^{13/10} \left( \frac{\alpha}{0.1} \right)^{9/5} \left( \frac{M}{M_\odot} \right)^{6/5} \text{ g s}^{-1} \quad (2.11)$$

have  $t_n < t_a$  and achieve the equilibrium  $Y_e$ ; this range covers the plausible  $\dot{M}$  for GRBs. Equation (2.11) as well as (2.7) and (2.10) apply to both Schwarzschild and Kerr black holes; the relativistic corrections alter the expressions only slightly. The main effect of the black hole spin enters simply by decreasing the characteristic radius  $r$  where most of accretion energy is liberated:  $r$  decreases from  $\sim 10r_g$  (Schwarzschild) to  $\sim r_g$  (Kerr).

The next question is very general: what is the equilibrium charged fraction  $Y_e$  of matter with given  $T$  and  $\rho$ ? The disk material should reach this  $Y_e$  as it is in thermodynamic, nuclear, and  $\beta$ -equilibrium. If the matter is transparent for neutrinos, the equilibrium  $Y_e$  is found by balancing the rates of reactions (2.6).<sup>9),10)</sup> The result is shown in Fig. 1, and a simple analytical calculation shows that  $Y_e < 0.5$  if  $\mu > Q/2$  where  $Q = (m_p - m_n)c^2$ . If the matter is opaque to neutrinos,  $Y_e$  is found by balancing the chemical potentials  $\mu + \mu_p = \mu_n + \mu_\nu$ . Then  $Y_e < 0.5$  if  $\mu > Q$ .

One concludes that accretion disks with  $\mu > Q$  should have a neutron excess

$n_n > n_p$ . This condition translates to a condition for  $\dot{M}$ ,<sup>9)</sup>

$$\dot{M} > \dot{M}_n \approx 10^{31} \left( \frac{r}{3r_g} \right)^{3/2} \left( \frac{\alpha}{0.1} \right) \left( \frac{M}{M_\odot} \right)^2 \text{ g s}^{-1}. \quad (2.12)$$

Plausible  $\dot{M}$  in GRB accretion flows are  $10^{32}$  g/s and higher, and they should be neutron rich. This turns out important for the overall picture of the GRB explosion.

### §3. Nuclear Composition of GRB Fireballs

The baryonic component of the jet is picked up from the turbulent accretion disk and remembers the disk  $Y_e$ , i.e. the jet has a lot of neutrons. The only threat to the escaping neutrons is the neutrino flux from the disk. The timescale for  $\nu$  absorption by  $n$  (and  $\bar{\nu}$  absorption by  $p$ ) is shorter than the escape timescale if the neutrino luminosity  $L_\nu > 10^{53}$  erg/s. In that case, the neutrino flux controls  $Y_e$  of the jet, which again is likely to give a neutron excess<sup>11),12)</sup> (although not necessarily<sup>9)</sup>), and  $Y_e$  freezes out quickly, at  $\sim 10$  Schwarzschild radii from the black hole.

The escaping jet is initially made of free nucleons  $n$  and  $p$ ,  $e^\pm$  pairs, radiation, and magnetic field. The jet expands and cools adiabatically, so that its internal energy is converted into bulk kinetic energy. When temperature drops to  $\approx 10^2$  keV the free nucleons tend to recombine into  $\alpha$ -particles, i.e. nucleosynthesis is expected. The situation is very much similar to the big bang nucleosynthesis: in both cases we deal with adiabatic expansion of radiation-dominated blackbody plasma. However, the outcome of nucleosynthesis turns out to be different.<sup>9),13),14)</sup>

Both the big bang and the GRB fireball can be described by three physical parameters: photon-to-baryon ratio  $\phi = n_\gamma/n_b$ , expansion timescale during the nucleosynthesis  $t_*$  (measured in the comoving frame), and  $Y_e$ , see the table below. The table also shows the characteristic nucleosynthesis temperature  $T_*$  and the ratio of the recombination rate to the expansion rate at  $T_*$ . This ratio is  $\sim 1$  for GRBs, which implies a marginally efficient nucleosynthesis, and the outcome depends on the precise values of parameters. An example is shown in Figure 2 with  $\phi = 10^5$ ,  $r_0/c = 10^{-4}$  s,  $Y_e = 0.5$ . The fireball is assumed to expand radially in this example. A realistic GRB jet can be non-radial: it can be collimated by a parabolic funnel of the rotating and collapsing star or by its own magnetic field.<sup>15)</sup> The nuclear reactions in a collimated jet have also been calculated.<sup>9)</sup> The collimation generally helps nucleosynthesis because it increases the expansion timescale, and then a significant fraction of nucleons recombine into  $\alpha$ -particles.

	$\phi = n_\gamma/n_b$	expansion timescale $t_*$	$Y_e$	$T_*$	$\frac{\text{recombination rate}}{\text{expansion rate}}$
Big Bang	$10^{10}$	$10^2$ s	$7/8$	80 keV	$\sim 10$
GRB	$10^5$	$10^{-4}$ s	$< 1/2$	140 keV	$\sim 1$

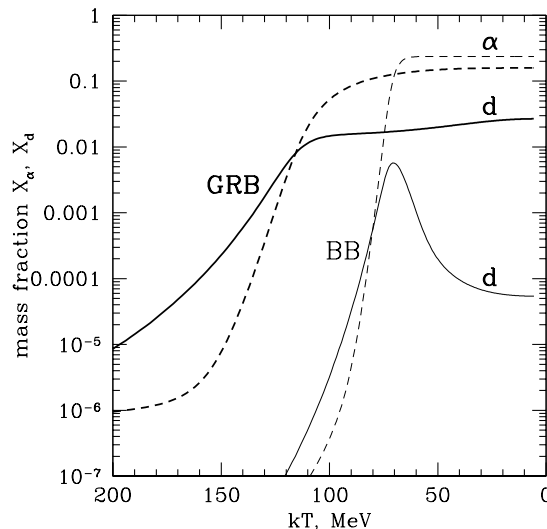


Fig. 2. Evolution of deuterium ( $d$ ) and helium ( $\alpha$ ) abundances with temperature in an expanding fireball. The (thicker) GRB curves are calculated for a radial explosion with  $\phi = n_\gamma/n_b = 10^5$ ,  $Y_e = 0.5$  and  $r_0 = 3 \times 10^6$  cm. For comparison, the big bang (BB) nucleosynthesis is also shown (with  $\phi = 3 \times 10^9$ ).

Even at conditions extremely favorable for nucleosynthesis, when the recombination rate is much higher than the expansion rate, there are leftover neutrons in the fireball because of the neutron excess  $Y_e < 0.5$  (the formation of  $\alpha$ -particles consumes equal numbers of  $n$  and  $p$ ). The mass fraction of leftover neutrons is then  $X_n = 1 - 2Y_e$ . For a similar reason, there are leftover protons in the big bang nucleosynthesis where  $Y_e \approx 7/8 > 0.5$ ; the mass fraction of leftover protons  $X_p = 1 - 2(1 - Y_e) = 3/4$  defines the hydrogen fraction of the observed universe, and the remaining  $1/4$  is made of the recombined nucleons (predominantly  $\alpha$ -particles and a tiny fraction of other light elements). By contrast, the post-nucleosynthesis GRB fireball is most likely composed of neutrons and  $\alpha$ -particles. Another interesting difference from the big bang is the large amount of deuterium in the freezeout (Fig. 2).

#### §4. Decoupling of Neutrons

The fireball is accelerated by the radiation pressure and its Lorentz factor  $\Gamma$  grows as long as  $aT^4 > n_b m_p c^2$ , where  $n_b$  is baryon density in the comoving frame. The neutron component practically does not participate in electromagnetic interactions, however, the neutrons also accelerate because they are collisionally coupled (via strong interactions) to the ions. The collisional timescale  $t_{\text{coll}}$  at small radii is very short compared to the fireball expansion timescale  $R/c$ , and the neutron Lorentz factor  $\Gamma_n$  only slightly lags behind the ion Lorentz factor  $\Gamma$ :

$(\Gamma - \Gamma_n)/\Gamma = t_{\text{coll}}c/R < 1$ .<sup>16)</sup> During the fireball acceleration,  $n_b$  scales as  $\Gamma^{-3}$  and the neutrons decouple ( $t_{\text{coll}}c/R > 1$ ) before the acceleration ends if  $\Gamma$  reaches  $\Gamma_{\text{dec}}$

$$\Gamma_{\text{dec}} \approx \left( \frac{\sigma_0 \dot{M}_\Omega}{m_p c r_0} \right)^{1/3} \approx 300 \left( \frac{\dot{M}_\Omega}{10^{26} \text{ g s}^{-1}} \right)^{1/3} \left( \frac{r_0}{3 \times 10^6 \text{ cm}} \right)^{-1/3}. \quad (4.1)$$

Here  $\sigma_0 \approx 3 \times 10^{-26} \text{ cm}^2$  describes the neutron-ion collisions,  $r_0$  is the size of the central engine, and  $\dot{M}_\Omega$  is the outflow rate of baryonic rest mass per unit solid angle. In radially expanding fireballs,  $\Gamma(R) = R/r_0$ ; this gives the decoupling radius  $\Gamma_{\text{dec}} r_0 \sim 10^9 \text{ cm}$ . Magnetically collimated fireballs can be non-radial out to very large radii,<sup>15)</sup> then  $\Gamma_{\text{dec}}$  can be one order of magnitude smaller.

Before the decoupling, the small relative velocity of the neutron fluid with respect to the ions,  $\beta_{\text{rel}} = t_{\text{coll}}c/R < 1$ , leads to a significant heating of the fireball. The neutron component has the kinetic energy  $E_{\text{rel}} = M_n c^2 \beta_{\text{rel}}^2 / 2$  in the ion fireball frame, which is dissipated on a short timescale  $t_{\text{coll}}$ . On the other hand,  $\beta_{\text{rel}}$  is constantly pumped by the acceleration of the fireball frame. The dissipation is similar to Ohmic heating in a conductor. Instead of electric current driven by an electric field, here the inertial “neutron current” is caused by acceleration of the fireball frame. Since the acceleration is driven by radiation, the dissipation in essence converts a fraction of the radiation energy into the thermal energy of baryons.

The baryonic component is heated with rate  $E_{\text{rel}}/t_{\text{coll}} = (1/2)M_n c^2 (t_{\text{coll}}c^2/R^2)$ . If the heat remained stored in the baryons, the baryonic temperature  $T_b (= T_{\text{ion}} = T_n)$  would be  $\approx m_p c^2 \beta_{\text{rel}}$ . However, the ions are thermally coupled to the electrons by Coulomb collisions, which are in turn coupled to radiation by Compton scattering. Therefore, most of the dissipated heat flows back to radiation, which strongly dominates the heat capacity of the fireball ( $n_\gamma/n_b \sim 10^5$ ). Only a fraction of the dissipated heat is kept by baryons to maintain  $T_b$  sufficiently high above  $T = T_e = T_\gamma$  so that the quasi-steady energy circulation is maintained in the accelerating fireball: radiation  $\rightarrow E_{\text{rel}} \rightarrow$  baryonic heat  $\rightarrow$  radiation.

The baryonic temperature  $T_b$  is found by equating the heating rate to the rate of Coulomb exchange between the ions and electrons. For radial fireballs ( $\Gamma = R/r_0$ ) this gives

$$T_b \approx 10^{10} \left( \frac{\Gamma}{\Gamma_{\text{dec}}} \right)^{9/2} \left( \frac{\dot{M}_\Omega}{10^{26} \text{ g s}^{-1}} \right)^{-1/2} \left( \frac{r_0}{3 \times 10^6 \text{ cm}} \right)^{1/2} \left( \frac{T_0}{10^{10} \text{ K}} \right)^{3/2} \text{ K}, \quad (4.2)$$

where  $T_0 = T(r_0)$  is the initial temperature of the fireball near the central engine. This expression is valid at  $\Gamma > (1/3)\Gamma_{\text{dec}}$  where  $T_b > T_0/\Gamma = T$ .  $T_b$  reaches values  $\sim 10^{10} \text{ K}$ , which is  $10^2 - 10^3$  times higher than it would be in the absence of neutrons: a fireball without neutrons would be in the blackbody state with  $T_b = T = T_0/\Gamma$ .

When  $t_{\text{coll}}$  approaches  $R/c$  the neutrons decouple from the ions. If the ion fireball is still accelerated by radiation at this moment, the relative velocity of neutrons approaches the speed of light and their last collisions with the ions are very energetic, above the threshold for pion production. The produced pions decay into muons, which in turn decay into electrons and neutrinos. Thus, an observable flux of multi-GeV neutrinos is produced.<sup>16), 17)</sup>



### §5. $\beta$ -Decay Inside the Fireball in the Prompt Emission Phase

After the decoupling, the neutrons coast with a constant Lorentz factor  $\Gamma_n = \text{const}$ . The ion fireball with energy  $\eta m_p c^2$  per baryon accelerates to  $\Gamma = \eta$  and, if  $\eta > \Gamma_{\text{dec}}$ , the final result of acceleration is  $\Gamma > \Gamma_n = \Gamma_{\text{dec}}$ . The fireball is then composed of two non-interacting components with different Lorentz factors.

The neutron component of total mass  $M_n$  gradually decays with rate  $\dot{M}_n = M_n c / R_\beta$  where

$$R_\beta = c\tau_\beta\Gamma_n = 8 \times 10^{15} \left( \frac{\Gamma_n}{300} \right) \text{ cm} \quad (5.1)$$

is the mean decay radius and  $\tau_\beta \approx 900$  s is the mean life-time of neutrons in their rest frame. At radii  $R < R_\beta$  the amount of decayed neutrons  $\Delta M_n = (R/R_\beta)M_n$  is small, however, their impact on the fireball can be significant if  $\Gamma > \Gamma_n$ . Then the charged products of  $\beta$ -decay  $p$  and  $e^-$  have a significant Lorentz factor with respect to the ion fireball,  $\Gamma_{\text{rel}} \sim \Gamma/\Gamma_n$ , and they immediately share their momentum as the two-stream plasma instability damps the relative motion on a short timescale.<sup>\*)</sup> The momentum exchange between the decayed neutrons and the ions is described as inelastic collision that heats up and decelerates the ion fireball. Calculations<sup>18)</sup> show that at radii  $10^{14} - 10^{16}$  cm the ion temperature rises to  $10^{11} - 10^{12}$  K and the ion  $\Gamma$  decreases.

Internal shocks are thought to occur in the fireball at about the same radii. The shocks develop because  $\eta$  is likely inhomogeneous in the fireball and different parts of it coast with different  $\Gamma$ . The shocks have been proposed as a mechanism of the prompt GRB emission. The heating and deceleration of the high- $\Gamma$  parts of the fireball by  $\beta$ -decay should reduce their Mach number. As a result, the amplitude of internal shocks is reduced or even suppressed completely, and this gives the most constraining upper bound on their efficiency.<sup>18)</sup>

### §6. $\beta$ -Decay in the Afterglow Phase

The  $\beta$ -decay depletes exponentially the neutron component outside the mean-decay radius  $R_\beta \approx 10^{16}(\Gamma_n/300)$  cm, which is comparable to the radius of the early afterglow emission. It turns out that the neutrons have a huge impact on the external blast wave at radii significantly larger than  $R_\beta$ , even though their number is exponentially reduced.

At typical afterglow radii  $10^{16} - 10^{17}$  cm the fireball can be viewed as a very thin shell (thickness  $\Delta \sim 10^{11}$  cm  $\ll R$ ). The survived neutron component coasts with a constant  $\Gamma_n$  while the ion component is decelerated by the external medium and eventually lags behind the neutrons. When  $\Gamma$  of the ions drops below  $\sim (R/\Delta)^{1/2} \sim$  a few hundred, the fireball splits into two distinct shells: the leading neutrons and the trailing ions.

---

<sup>\*)</sup> Another, and likely dominant, mechanism of momentum sharing is the gyration of the decay products in a transverse magnetic field frozen in the fireball (the transverse component is dominant in a radially expanding plasma as follows from magnetic flux conservation).

The front of survived neutrons overtakes the decelerating external shock wave at radius  $R_*$  where the shock-wave Lorentz factor  $\Gamma$  decreases below  $\Gamma_n$ . Using the Blandford-McKee solution  $\Gamma^2(R) = (17 - 4k)E/8\pi\rho_0c^2R^3$  for adiabatic blast waves in a medium with density  $\rho_0 \propto R^{-k}$  we find  $R_*$  from equation

$$R_*^3\rho_0(R_*) = \frac{(17 - 4k)E}{8\pi c^2\Gamma_n^2}. \quad (6.1)$$

A typical afterglow model with  $\rho_0 = \text{const} \sim 10^{-24} \text{ g cm}^{-3}$ ,  $E \sim 10^{52} \text{ erg}$ , and  $\Gamma_n \approx 300$ , gives  $R_* \sim 3 \times 10^{16} \text{ cm}$ . At  $R > R_*$  the  $\beta$ -decay takes place in the external medium *ahead* of the forward shock that produces the afterglow radiation.

The impact of this decay can be understood by comparing the energy of neutrons,  $E_n \approx X_n E \exp(-R/R_\beta)$  ( $X_n$  is the initial neutron fraction of the explosion) with the ambient mass  $mc^2 = \frac{4\pi}{(3-k)}R^3\rho_0c^2 = \frac{(17-4k)}{2(3-k)}(E/\Gamma^2)$  they interact with,

$$\frac{E_n}{mc^2} = \frac{2(3-k)}{17-4k}X_n\Gamma^2 \exp\left(-\frac{R}{R_\beta}\right). \quad (6.2)$$

Immediately after  $R_*$  this ratio can be as large as  $\Gamma_n^2 \sim 10^5$ , depending on  $R_*/R_\beta$ . The decaying neutron front with  $E_n > mc^2$  deposits huge momentum and energy into the ambient medium, leaving behind a relativistic trail. The exact parameters of this trail are found from energy and momentum conservation.<sup>20)</sup>

The ratio  $E_n/mc^2$  decreases to unity after  $\approx 10$  e-foldings of  $\beta$ -decay. Therefore the impact of neutrons lasts until  $R_{\text{trail}} \approx 10R_\beta \approx 10^{17} \text{ cm}$ , and one expects an observational effect if  $R_* < R_{\text{trail}}$ . For homogeneous medium ( $k = 0$ ) this requires a number density  $n_0 > 0.1E_{52}(\Gamma_n/300)^{-5} \text{ cm}^{-3}$ . For wind-type models ( $k = 2$ )  $R_* < R_{\text{trail}}$  for all plausible parameters of the wind if  $\Gamma_n \sim 10^2$  or higher.\*)

The  $\beta$ -decay ahead of the shock transforms the cold static external medium into a hot, dense, relativistically moving, and possibly magnetized, material. This transformation of the preshock medium should affect the appearance of the afterglow radiation. Like the neutron-free shocks, it is difficult to calculate the emission from first principles because the electron acceleration and magnetic field evolution are poorly understood. The best one could do is to apply a phenomenological shock model with customary parameters  $\epsilon_e$  and  $\epsilon_B$ :  $\epsilon_e$  is the fraction of shock energy passed to the nonthermal electrons and  $\epsilon_B$  is the energy fraction in postshock magnetic field. This may enable an observational test for the  $\beta$ -decay in the afterglow phase.

## §7. Conclusions

The GRB phenomenon can be associated with formation of stellar-mass black holes with small-scale disks of dense material that accretes quickly and produces a relativistic jet. The neutronization process takes place in the disk and, as a result, the baryonic component of the jet is neutron rich. The observed explosion then

\*) Besides, the forward shock in the dense wind of a Wolf-Rayet progenitor is likely to be slow from the very beginning (the reverse shock in the ejecta is relativistic,  $\Gamma_{\text{ej}} \gg \Gamma$ ). Then  $\Gamma < \Gamma_n$  and the neutrons overtake the shock immediately, before the self-similar deceleration sets in.

resembles a huge neutron bomb. The jet accelerates to Lorentz factors  $10^2 - 10^3$ , so the decay time of neutrons is increased by the factor  $10^2 - 10^3$  and an interesting fraction of neutrons survive out to large distances  $\sim 10^{17}$  cm. Such distances cover the prompt phase of  $\gamma$ -ray emission and at least the early afterglow. The survived fraction of neutrons should overtake the external shock wave and deposit huge energy in the ambient medium, thus changing the very mechanism of the GRB blast wave.

Relativistic neutron outflows were also proposed to take place in AGN.<sup>21)</sup> They originated from nonthermal protons in accretion disks around supermassive black holes and decayed far away in the ambient medium. In contrast to GRBs, the AGN neutron outflows are steady and uncollimated. The GRB neutrons have a better chance to be observed as they affect the observed development of the explosion.

Any neutron signature revealed in a GRB afterglow emission would confirm that the ejected baryonic material has gone through a hot high-density phase in the central engine. Neutrons thus provide a unique link between the physics of the central engine and the observed afterglow. Numerical simulations of neutron-fed blast waves may help to identify such signatures. One possibility, for instance, is an exponentially decaying emission component. Another possible signature is a spectral transition or a bump in the afterglow light curve at  $R \approx R_{\text{trail}}$ .<sup>20)</sup>

Absence of neutron signatures would indicate that the GRB jets are dominated by magnetic fields. In such a low- $\dot{M}_{\text{O}}$  jet, neutrons would decouple early with a modest Lorentz factor (eq. 4.1) and decay quickly. A two-component jet with less collimated and less energetic neutrons is possible in the MHD acceleration scenario.<sup>15)</sup>

### Acknowledgements

This research was supported by NASA grant NAG5-13382.

### References

- 1) Y. Lithwick and R. Sari, *ApJ*, **555** (2001), 540.
- 2) P. Mészáros, *ARAA*, **40** (2002), 137.
- 3) K.Z. Stanek et al., *ApJ*, **591** (2003), L17.
- 4) D. Proga, A.I. MacFadyen, P.J. Armitage, and M.C. Begelman, *ApJ*, **599** (2003), L5
- 5) Y. Mizuno, S. Yamada, S. Koide, and K. Shibata, *ApJ*, submitted (astro-ph/0404152)
- 6) R. Popham, S.E. Woosley, and C. Fryer, *ApJ*, **518** (1999), 356.
- 7) R. Narayan, T. Piran, and P. Kumar, *ApJ*, **557** (2001), 949.
- 8) K. Kohri, and S. Mineshige, *ApJ*, **577** (2002), 311.
- 9) A.M. Beloborodov, *ApJ*, **588** (2003), 931.
- 10) J. Pruet, S.E. Woosley, & R.D. Hoffman, *ApJ*, **586** (2003), 1254.
- 11) Y.-Z. Qian, G.M. Fuller, G.J. Mathews, R.W. Mayle, J.R. Wilson, and S.E. Woosley, *Phys. Rev. Lett.*, **71** (1993), 1965.
- 12) J. Pruet, G.M. Fuller, and C.Y. Cardall *ApJ*, **561** (2001), 957.
- 13) M. Lemoine, *A&A*, **390** (2002), L31.
- 14) J. Pruet, S. Guiles, and G.M. Fuller, *ApJ*, **580** (2002), 368.
- 15) N. Vlahakis, F. Peng, and A. Königl, *ApJ*, **594** (2003), L23.
- 16) E.V. Derishev, V.V. Kocharovsky, and V.I. Kocharovsky, *ApJ*, **521** (1999), 640.
- 17) J.N. Bahcall and P. Mészáros, *Phys. Rev. Lett.*, **85** (2000), 1362.
- 18) E.M. Rossi, A.M. Beloborodov, and M.J. Rees (2004) in preparation
- 19) R.D. Blandford and C.F. McKee, *Phys. Fluids*, **19** (1976), 1130.
- 20) A.M. Beloborodov, *ApJ*, **585** (2003), L19.
- 21) M. Sikora, M.C. Begelman, and B. Rudak, *ApJ*, **341** (1989), L33